British Journal of Pharmacology

RESEARCH PAPER

Towards functional selectivity for α6β3γ2 GABA_A receptors: a series of novel pyrazoloquinolinones

Correspondence Margot Ernst, Department of Molecular Neurosciences, Center for Brain Research, Medical University Vienna, Spitalgasse 4, 1090 Vienna, Austria. E-mail: margot.ernst@meduniwien.ac.at

Marco Treven[1],*, David C B Siebert[2],* (iD), Raphael Holzinger[1], Konstantina Bampali[1], Jure Fabjan[1], Zdravko Varagic[1], Laurin Wimmer[2], Friederike Steudle[3], Petra Scholze[3], Michael Schnürch[2], Marko D Mihovilovic[2] and Margot Ernst[1] (iD)

[1]*Department of Molecular Neurosciences, Center for Brain Research, Medical University Vienna, Vienna, Austria,* [2]*Institute of Applied Synthetic Chemistry, TU Wien, Vienna, Austria, and* [3]*Department of Pathobiology of the Nervous System, Center for Brain Research, Medical University Vienna, Vienna, Austria*

*These authors contributed equally to this study.

BACKGROUND AND PURPOSE

The GABA_A receptors are ligand-gated ion channels, which play an important role in neurotransmission. Their variety of binding sites serves as an appealing target for many clinically relevant drugs. Here, we explored the functional selectivity of modulatory effects at specific extracellular α+/β− interfaces, using a systematically varied series of pyrazoloquinolinones.

EXPERIMENTAL APPROACH

Recombinant GABA_A receptors were expressed in *Xenopus laevis* oocytes and modulatory effects on GABA-elicited currents by the newly synthesized and reference compounds were investigated by the two-electrode voltage clamp method.

KEY RESULTS

We identified a new compound which, to the best of our knowledge, shows the highest functional selectivity for positive modulation at α6β3γ2 GABA_A receptors with nearly no residual activity at the other αxβ3γ2 (*x* = 1–5) subtypes. This modulation was independent of affinity for α+/γ− interfaces. Furthermore, we demonstrated for the first time a compound that elicits a negative modulation at specific extracellular α+/β− interfaces.

CONCLUSION AND IMPLICATIONS

These results constitute a major step towards a potential selective positive modulation of certain α6-containing GABA_A receptors, which might be useful to elicit their physiological role. Furthermore, these studies pave the way towards insights into molecular principles that drive positive versus negative allosteric modulation of specific GABA_A receptor isoforms.

Abbreviations

BZD, benzodiazepine; CGC, cerebellar granule cells; PAM, positive allosteric modulation; PQ, pyrazoloquinolinone

Introduction

Pyrazoloquinolinones (PQs) have been studied since the 1980s for their benzodiazepine (BZD) receptor affinity (Yokoyama *et al.,* 1982). The prototypical PQ, **CGS8216** (all residues = H; see scaffold in Figure 1), displaced [³H]-flunitrazepam and [³H]-diazepam binding at subnanomolar concentrations (Czernik *et al.,* 1982), was devoid of *in vivo* BZD-like activity (Gee and Yamamura, 1982) and showed proconvulsant actions in mice (File, 1983). Residue modifications led to varying neurochemical and behavioural properties. For example, compound **1** (CGS9895; R'^4 = methoxy; see Figure 1) (Ramerstorfer *et al.,* 2011; Varagic *et al.,* 2013b) not only antagonized the effects of diazepam but also showed anxiolytic and weak anticonvulsant activity while being devoid of sedation, muscle relaxation or motor impairments (Bennett *et al.,* 1985; Bennett, 1987). These findings encouraged the possibility of separately eliciting only specific desired BZD-like effects (Kolata, 1982). Early on, researchers noted a dissociation between BZD receptor activity and the *in vivo* pharmacology of PQs (Bennett, 1987; Cooper *et al.,* 1987).

The most abundant **GABA_A receptor** types are composed of one γ2, two α and two β subunits, forming pentameric GABA-gated chloride channels (Olsen and Sieghart, 2008). They are modulated by several allosteric ligand binding sites (Puthenkalam *et al.,* 2016), including the BZD binding site at extracellular α+/γ− interfaces (Sigel, 2002; Ernst *et al.,* 2003), and a modulatory PQ binding site at α+/β− interfaces (Ramerstorfer *et al.,* 2011). The demonstration that PQs are high affinity null modulators at BZD binding sites and low potency allosteric modulators at modulatory PQ binding sites (Ramerstorfer *et al.,* 2011) helped explain their complex pharmacology and inspired a new search for GABA_A receptor subtype-specific modulators (Sieghart *et al.,* 2012). Importantly, compound **1** did not require BZD-site binding for its modulatory effects, as GABA current enhancements were almost identical in α1β3 versus α1β3γ2 receptors (Ramerstorfer *et al.,* 2011), as well as in α1β2 versus α1β2γ2 receptors (Maldifassi *et al.,* 2016), and obstructing the BZD-site with a steric hindrance approach did not diminish compound **1** current modulation in α1β3γ2 receptors (Ramerstorfer *et al.,* 2011). A recent study employing α1Y209 point mutations confirmed the modulatory PQ binding site (Maldifassi *et al.,* 2016).

GABA_A receptor α6 subunits are highly expressed in cerebellar granule cells (CGCs) (Hörtnagl *et al.,* 2013) and have long been studied for their presumed contribution to the intoxicating effects of ethanol (Valenzuela and Jotty, 2015). Recently, they gained additional interest as potential targets in pain, motor tic and depressive disorders (Puri *et al.,* 2012; Kramer and Bellinger, 2013; Liao *et al.,* 2016; Yang *et al.,* 2016).

Here, we expand on previously identified α6β3γ2 preferring ring PQs (Varagic *et al.,* 2013a) and present, to the best of our knowledge, the most effective selective compound for this subtype discovered so far, compound **3** (LAU159). A substituent variation to the *o*-methoxy [compound **4** (LAU165), see Figure 1 for nomenclature] completely abolishes the positive modulation at all αxβ3γ2 (*x* = 1–6)
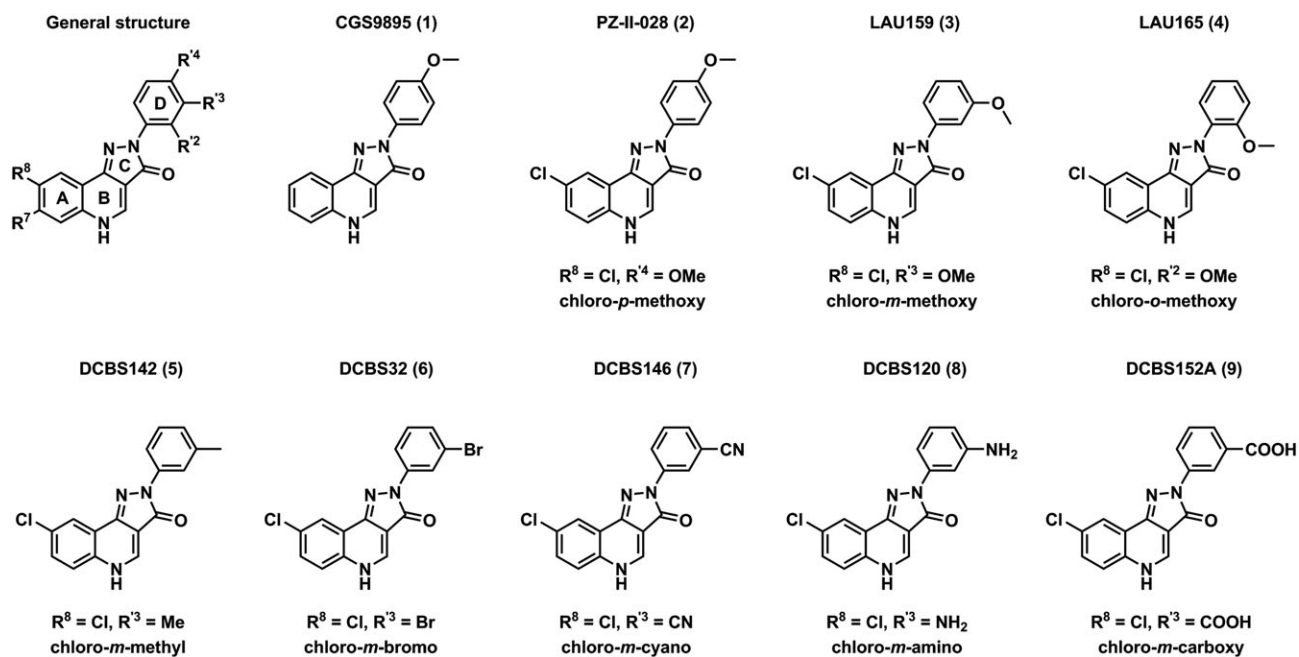
Figure 1

PQ structures. Top left: PQ scaffold with labels for rings A to D and residue numbering (R^7 and R^8 on ring A; R'^2 (*o*), R'^3 (*m*), R'^4 (*p*) on ring D). Top row: **1** is a *p*-methoxy compound with unsubstituted ring A. R^8 = chloro compounds are derived from varying the position of the methoxy group at ring D. Bottom row: compound variants with different residues in R'^3 *m*-position.

receptors, providing a potential negative control compound for future *in vivo* studies. Variation of the functional group in the *m*-position on ring D led to the first negative modulator (**9**) at the modulatory PQ site in some receptor isoforms.

Methods

Two-electrode voltage clamp electrophysiology

Preparation of mRNA for rat α1, α2, α3, α4, α5, α6, β3 and γ2 subunits and electrophysiological experiments with *Xenopus laevis* oocytes were performed as described previously (Forkuo *et al.*, 2016). Mature female *X. laevis* (Nasco, Fort Atkinson, WI, USA) were anaesthetized in a bath of ice-cold 0.17% Tricain (Ethyl-m-aminobenzoat, Sigma-Aldrich, St. Louis, MO, USA) before decapitation and transfer of the frog's ovary to ND96 medium (96 mM NaCl, 2 mM KCl, 1 mM MgCl2, 5 mM HEPES; pH 7.5). From a total of at most 35 toads, cells were used for this and other parallel studies, reflecting the total number of weeks of data collection. Tissue was obtained in accordance with the rules of the Austrian animal protection law and Austrian animal experiment by-laws, which implement European Directive 2010/63/EU and complies with the ARRIVE guidelines. Animal studies are reported in compliance with the ARRIVE guidelines (Kilkenny *et al.*, 2010; McGrath and Lilley, 2015). Following incubation in 1 mg·mL^{-1} collagenase (Sigma-Aldrich, St. Louis, MO, USA) for 30 min, stage 5 to 6 oocytes were dissected out of the ovary and defolliculated using a platinum wire loop or glass Pasteur pipette. Oocytes were stored and incubated at 18°C in NDE medium (96 mM NaCl, 2 mM KCl, 1 mM MgCl$_2$, 5 mM HEPES, 1.8 mM CaCl$_2$; pH 7.5) that was supplemented with 100 U·mL^{-1} penicillin, 100 μg·mL^{-1} streptomycin and 2.5 mM pyruvate. Oocytes were injected with an aqueous solution of mRNA. A total of 2.5 ng of mRNA per oocyte was injected. The subunit ratio was 1:1:5 for αxβ3γ2 (*x* = 1,2,3,5), and 3:1:5 for α4/α6β3γ2 receptors. In some cases, concatenated constructs were used (Minier and Sigel, 2004), which were a kind gift of E. Sigel. Specifically, cRNA coding for one triple concatemer γ2-β3-α6 was co-injected in oocytes with cRNA coding for one double concatemer β3-α6 in a 1:1 ratio, and currents confirmed to be equally modulated by PZ-II-029 as non-concatenated α6β3γ2. Injected oocytes were incubated for at least 36 h before electrophysiological recordings. Oocytes were placed on a nylon-grid in a bath of NDE medium. For current measurements, oocytes were impaled with two microelectrodes which were filled with 2 M KCl and had a resistance of 2–3 MΩ. The oocytes were constantly washed by a flow of 6 mL·min^{-1} NDE that could be switched to NDE containing GABA and/or drugs. Drugs were diluted in the NDE from DMSO solutions resulting in a final concentration of 0.1% DMSO. To test the effects of the compounds on the GABA-induced currents, a GABA concentration was titrated to trigger 3–5% of the respective maximum GABA-elicited current of the individual oocyte (EC$_{3–5}$) and was applied to the cell together with various concentrations of test compounds. All recordings were performed at room temperature at a holding potential of −60 mV using a Warner OC-725C two-electrode voltage clamp (TEV) (Warner Instrument, Hamden, CT, USA) or a Dagan CA-1B Oocyte Clamp or a Dagan TEV-200A TEV amplifier (Dagan Corporation, Mineapolis, MN, USA). Data were digitized using a Digidata 1322A or 1550 data acquisition system (Axon Instruments, Union City, CA, USA), recorded using Clampex 10.5 software (Molecular Devices, Sunnyvale, CA, USA), and analysed using Clampfit 10.5 and GraphPad Prism 6.0 (La Jolla, CA, USA) software. Concentration–response data were fitted using the Hill equation. Data are given as mean ± SEM from at least three oocytes from two batches.

Radioligand displacement assays

Radioligand displacement experiments were performed using 12- to 16-week-old female Sprague–Dawley rats (Institute of Biomedical Research, Medical University of Vienna, Himberg, Austria). In total, 10 rats were used. All animals were group housed (six animals per cage) at an ambient temperature of 21°C with a light : dark regime of 10:14 h, with *ad libitum* access to standard food and water. Rats were anaesthetized under CO$_2$ and decapitated in accordance with the Guidelines of the Animal Care Committee of the Medical University of Vienna. The brains were removed immediately, and cerebellar membranes were prepared as described previously (Sieghart and Schuster, 1984). Displacement assays using [^{3}H]-flunitrazepam were performed as described by Simeone *et al*. (2017). Displacement assays using [^{3}H]-Ro15-4513 were performed as follows: In brief, membrane pellets were incubated for 90 min at 4°C in a total of 500 μL of a solution containing 50 mM Tris/citrate buffer, pH = 7.1, 150 mM NaCl and 5 nM [^{3}H]Ro15-4513 in the presence of 50 μM diazepam (to saturate α1-containing receptors and target α6-containing receptors only) and in the absence or presence of either 100 μM Ro15-1788 (to determine non-specific binding) or various concentrations of receptor ligands (dissolved in DMSO, final DMSO-concentration 0.5%). Membranes were filtered through Whatman GF/B filters and washed twice with 4 mL of ice-cold 50 mM Tris/citrate buffer. Filters were transferred to scintillation vials and subjected to scintillation counting after the addition of 3 mL Rotiszint Eco plus liquid scintillation cocktail. Nonlinear regression analysis of the displacement curves used the equation: log(inhibitor) versus response – variable slope with Top = 100% and Bottom = 0% $Y = 100/(1 + 10^{\wedge}((logIC_{50}-x)*Hillslope))$.

Saturation binding experiments were performed by incubating the membranes with various concentrations of [^{3}H]-Ro15-4513 in the absence or presence of 50 μM diazepam and analysed using the equation $Y = B_{max}*X/(KD + X)$, and an equilibrium binding constant KD for rat cerebellum was determined (KD ± SEM n = 3 independent experiments): 1.4 ± 0.1 nM.

IC$_{50}$ values were converted to K_i values using the Cheng–Prusoff relationship $K_i = IC_{50}/(1 + (S/KD))$ with S being the concentration of the radioligand (5 nM) and the KD value described above (1.4 nM).

All analyses were performed using GraphPad Prism version 7 for PC, GraphPad Software, La Jolla, California, USA, www.graphpad.com.

Data and statistical analysis

All results are expressed as mean ± SEM. The n number stated represents the number of single oocyte experiments. In cases of inactivity, a number of $n = 2$ was considered as adequate, whereas statistical analysis was performed with a number of $n \geq 5$ only. Data were analysed with GrapdPad Prism 6.0 and evaluated with one-way ANOVA with Dunnett's multiple comparison test. The data and statistical analysis comply with the recommendations on experimental design and analysis in pharmacology (Curtis *et al.*, 2015).

Materials

Conformation analysis. Conformational analysis of pyrazoloquinolinone structures was performed using the Conformation Search application integrated in the MOE software [Molecular Operating Environment (MOE), Chemical Computing Group Inc., Montreal, QC, Canada].

Compound synthesis. Compounds **1** (CGS9895) and **2** (PZ-II-028) have been synthesized and published, recently. Synthesis of compounds **3** (LAU159), **4** (LAU165), **5** (DCBS142), **6** (DCBS32), **7** (DCBS146), **8** (DCBS120) and **9** (DCBS152A) was conducted in analogy to previously outlined synthetic routes (Fryer *et al.*, 1993; Savini *et al.*, 2001; Varagic *et al.*, 2013b) (see Supporting Information).

Compounds investigated. The following compounds were used: **3** (LAU159): 8-chloro-2-(3-methoxyphenyl)-2H,3H,5H-pyrazolo[4,3-c]quinolin-3-one; **4** (LAU165): 8-chloro-2-(2-methoxyphenyl)-2H,3H,5H-pyrazolo[4,3-c]quinolin-3-one; **5** (DCBS142): 8-chloro-2-(3-methylphenyl)-2H,3H,5H-pyrazolo-[4,3-c]quinolin-3-one; **6** (DCBS32): 2-(3-bromophenyl)-8-chloro-2H,3H,5H-pyrazolo[4,3-c]-quinolin-3-one; **7** (DCBS146): 3-(8-chloro-3-oxo-2H,3H,5H-pyrazolo[4,3-c]quinolin-2-yl)-benzonitrile; **8** (DCBS120): 2-(3-aminophenyl)-8-chloro-2H,3H,5H-pyrazolo[4,3-c]quinolin-3-one; **9** (DCBS152A): 3-(8-chloro-3-oxo-2H,3H,5H-pyrazolo[4,3-c]quinolin-2-yl) benzoic acid.

Nomenclature of targets and ligands

Key protein targets and ligands in this article are hyperlinked to corresponding entries in http://www.guidetopharmacology. org, the common portal for data from the IUPHAR/BPS Guide to PHARMACOLOGY (Southan *et al.*, 2016), and are permanently archived in the Concise Guide to PHARMACOLOGY 2017/18 (Alexander *et al.*, 2017).

Results

Impact of R^8 = chloro and of variations in the position of the ring D methoxy substitution on $GABA_A$ receptor subtype modulatory profile

Compound **1** positively modulates EC_{3-5} GABA currents (effective concentration eliciting 3–5% of maximum GABA currents) in all $\alpha x\beta 3\gamma 2$ ($x = 1$–6) subunit combinations (Ramerstorfer *et al.,* 2011) (see Figure 2A). Compound **1** shows higher modulatory efficacy for $\alpha 6\beta 3\gamma 2$ receptor currents, which are enhanced to roughly 700% at 10 μM compound concentration. The remaining $\alpha x\beta 3\gamma 2$ ($x = 1$–5) subunit

combinations are modulated to a lesser extent (see Figure 2 A). Interestingly, upon introduction of an R^8 = chloro residue, resulting in compound **2**, maximum modulations are enhanced by about threefold, while preserving relative modulatory strength between the tested subunit combinations (see Figure 2B). Compound **2** maximum modulation amounts to ~2000% in the case of $\alpha 6\beta 3\gamma 2$ receptor currents and reaches ~1000% at $\alpha 1\beta 3\gamma 2$ and $\alpha 2\beta 3\gamma 2$ receptors (see Figure 2B). The fitted curves suggest that the presence of R^8 = chloro does not induce a substantial left shift of the compound dose–response curves at any of the $\alpha x\beta 3\gamma 2$ ($x = 1$–6) subunit combinations. Systematic structural variants of compound **2** were subsequently synthesized (see Figure 1), in order to explore how chemically diverse ring D substitutions would affect efficacy and potency in different subtypes.

Changing the methoxy residue on ring D to the *m*-position (**3**) completely abolished $\alpha x\beta 3\gamma 2$ ($x = 1$–5) modulatory activity, while at $\alpha 6\beta 3\gamma 2$ around 300% modulation with an estimated EC_{50} of 3.1 μM remained (see Figure 2C). At 1 μM compound **3**, modulation amounted to 148.6 ± 10.5% [mean ± SEM, $n = 13$, control (GABA) = EC_{3-5}]. Compound **3**, while not acting as positive modulator in this subtype, still retained some affinity at the modulatory PQ site of $\alpha 1\beta 3\gamma 2$, as 10 and 30 μM reduced the modulatory effect of compound **2** (1 μM) at this receptor subtype (see Figure 2F) and thus is a null modulator in this subtype. Further moving the methoxy residue to the *o*-position (**4**) abolished any positive allosteric modulation (PAM) activity but led to weak negative modulatory activity at $\alpha 5\beta 3\gamma 2$ (see Figure 2D).

Compound **4** does not bind at the $\alpha 6+/\beta 3-$ interface

Analogously to compound **3** at $\alpha 1\beta 3\gamma 2$ (see Figure 2F), the lack of modulatory activity of compound **4** at $\alpha 6\beta 3\gamma 2$ (see Figure 2D) could mean that it is either a silent binder or a non-binder at the $\alpha 6+/\beta 3-$ modulatory PQ binding site. This cannot be determined using binding assays, because no radioactively labelled ligand with specificity for any of the modulatory $\alpha+/\beta-$ PQ sites is currently available. We therefore tested whether effects of compound **3** at $\alpha 6\beta 3\gamma 2$ receptors can be inhibited by co-application of compound **4**. Up to 30 μM, compound **4** (which is the solubility limit in the assay buffer) was unable to abolish the modulatory effect elicited by compound **3** (3 μM) in this series (see Figure 3A, B).

Based on these results, we asked how the methoxy residue in *o*-position could possibly interfere with biological activity. The biological effect of a compound may not always arise from the conformation which is the energetic global minimum (of compound alone), or from only one conformation, but rather from an ensemble of conformations. We therefore performed a conformational analysis using the conformation search application provided by the MOE software package. Since pyrazoloquinolinones are quite inflexible, we focused on the dihedral angle (φ) between the two plane surfaces of the rings A–C and ring D (see Figure 4). According to this analysis, the *p*- and *m*-methoxy substituted compounds possess one main conformation which displays co-planarity between rings A–C and ring D (φ = ~0.003° and φ = ~0.03°), whereas the *o*-methoxy substitution features 2 possible
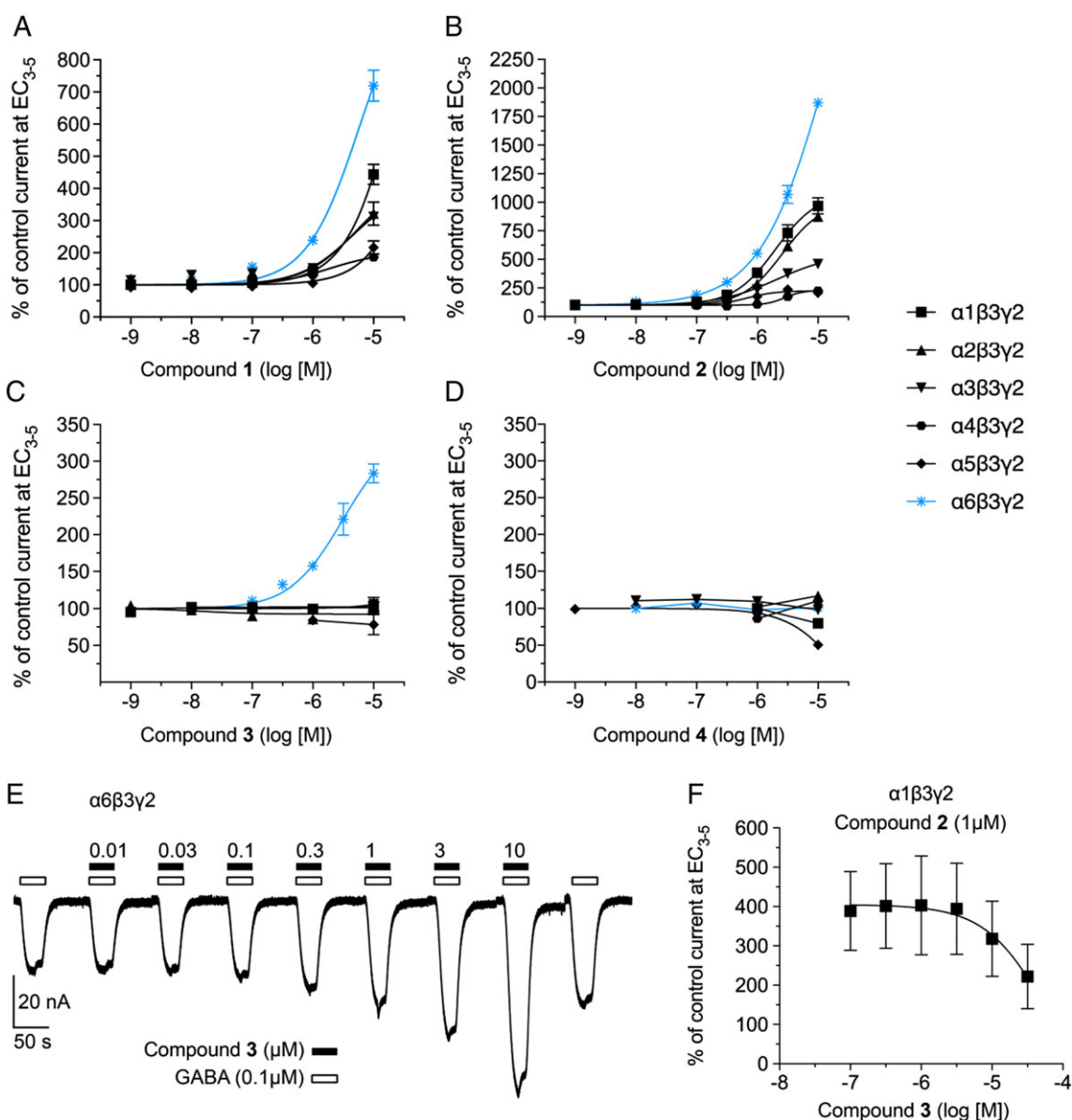
Figure 2

(A–D) GABAA receptor subtype activity profile of compounds with systematically varying positions of the methoxy-group on ring D (compound **1**, compound **2**: *p*-methoxy; compound **3**: *m*-methoxy; compound **4**: *o*-methoxy) at αxβ3γ2 (*x* = 1–6) GABAA receptors. Y-axis shows % modulation of currents elicited by a GABA concentration amounting to 3–5% of maximum GABA currents per cell. For the purpose of structure–activity comparison, some datasets are reproduced: compound **1** at αxβ3γ2 (*x* = 1,2,3 and 5) reproduced with permission (Ramerstorfer *et al.*, 2011). Compound **2** at αxβ3γ2 (*x* = 1–6) reproduced with permission (Varagic *et al.*, 2013a). (E) Sample recording of GABA currents and co-application of increasing concentrations of compound **3**, from an oocyte injected with α6β3γ2 subunits. (F) Co-application of compound **3** (10 and 30 μM) can inhibit positive GABA current modulation by 1 μM of compound **2**.

conformations (syn and anti, see Supporting Information Figure S3). While the anti-conformation shows already 0 to 200 times stronger rotation between the plane surfaces, the syn-conformation leads to a significant rotation of the ring D up to a dihedral angle of 20° (see Figure 4C and Supporting Information Table S1). This rotation of ring D might be a reasonable explanation for the loss of activity of compound **4**.

Since pyrazoloquinolinones are also high-affinity ligands at the benzodiazepine binding site (Ramerstorfer *et al.*, 2011),

we next performed radioligand displacement assays for compounds **2**, **3** and **4** in cerebellar membranes, to determine their affinities at α1+/γ2− and α6+/γ2− sites (see Supporting Information Table S4). The results show that the tested compounds are high to very high affinity binders at the α1+/γ2− BZ site and moderate to high affinity binders at the diazepam-insensitive α6+/γ2− BZ site. Furthermore, we observed a decrease of affinity when changing the substituent from the *p*- to the *o*-position in α1+/γ2− and in α6+/γ2−.
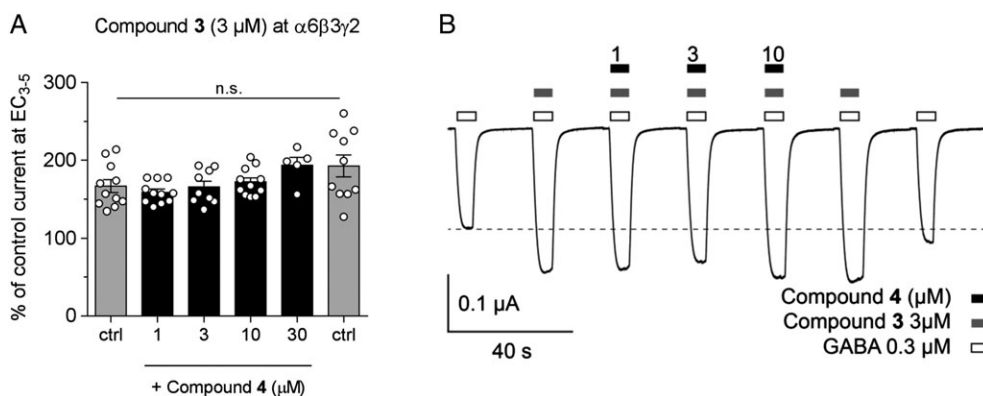
Figure 3

Compound **4** is unable to block modulatory effects of compound **3** at α6β3γ2. (A) Modulation by compound **3** (3 µM) is unaffected by co-application of compound **4** (n.s. = not significant; $n = 9$; $P > 0.05$ all groups vs. control before, one-way ANOVA with Dunnett's multiple comparison test). (B) Sample recording of one oocyte sequentially exposed to 3 µM of compound **3** + increasing concentrations of compound **4** (one experiment from data presented in A).
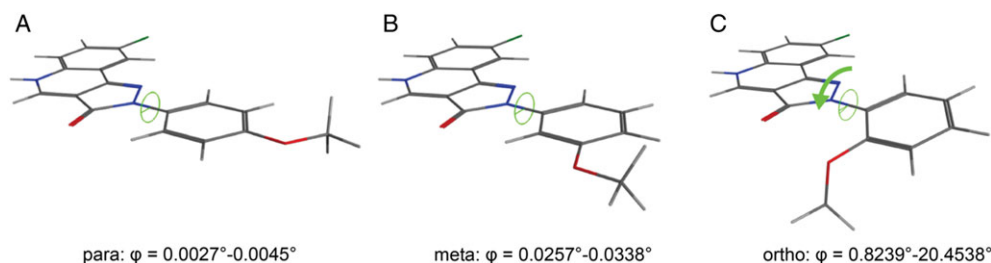
Figure 4

Conformational analysis of compounds **2** (A), **3** (B) and **4** (C). Position of the methoxy substituent on ring D influences the dihedral angle φ between the planes of rings A–C and ring D. Number of calculated conformations: $P = 2$, $m = 3$, $o = 4$ (see Supporting Information Table S1). Methoxy substitution in o-position rotates ring D by up to ~20° (green arrow).

R^8 = chloro compounds with varying m-substituents on ring D display distinct efficacy profiles

The remarkable α6β3γ2 selectivity of m-methoxy compound **3** spurred us to screen additional compounds with varying m-substituents (see Figure 1, bottom row), for their modulatory activity at α6β3γ2 receptors (see Figure 5A). Two of these, compound **5** (DCBS142) and compound **9** (DCBS152A), displayed similar or higher modulatory activity at 1 µM concentration at α6β3γ2 compared to compound **3** (see Figure 5A) and were thus investigated further for their α-selectivity profile (see Figure 5B, C). Neither of them was found to be selective for any tested receptor subtype. Selectivity of relevant compounds for α6β3γ2 over α1β3γ2 is quantified in Figure 5D, in comparison to PZ-II-029 (Varagic et al., 2013a), the most α6β3γ2 selective compound until now; 10 µM compound **5** positively modulated α1β3γ2 to 210.7 ± 17% [mean ± SEM, $n = 4$, control (GABA) = $EC_{3–5}$], and the other tested subtypes to a lesser extent. Thus, the subtype profile of compound **5** is reminiscent of compound **1**. In contrast, m-carboxy compound **9** is a negative modulator at several subtypes, particularly at α1β3γ2, where 10 µM compound **9** reduced GABA responses to 17.9 ± 7.4% [mean ± SEM, $n = 4$, control (GABA)- = $EC_{3–5}$] (see Figure 5B, C). Thus, compound **9** displays bi-directional modulatory effects depending on the α subunit present. The modulation of α1β3γ2 by compounds **5** and **9** did not require the presence of a γ2 subunit (Ramerstorfer et al., 2011), as modulatory effects in α1β3γ2 and α1β3 were overlapping in both cases (see Figure 5E).

The finding that the presence of a γ2 subunit did not affect modulation by compounds **5** and **9** (see Figure 5E) prompted us to investigate the functional selectivity profile of compound **3** with respect to a third subunit. Since Jechlinger et al. (1998) reported that α6βγ2 and α6βδ are populations of comparable size, we thus aimed to investigate compound **3** in α1,4,6β3δ receptors subtypes (see Supporting Information Table S5). In line with the data for compounds **5** and **9**, we noticed for compound **3** that the presence of a γ2 subunit did not affect current modulation. Moreover, we even observed a comparable functional selectivity for the α6-containing αβδ receptor subtype.
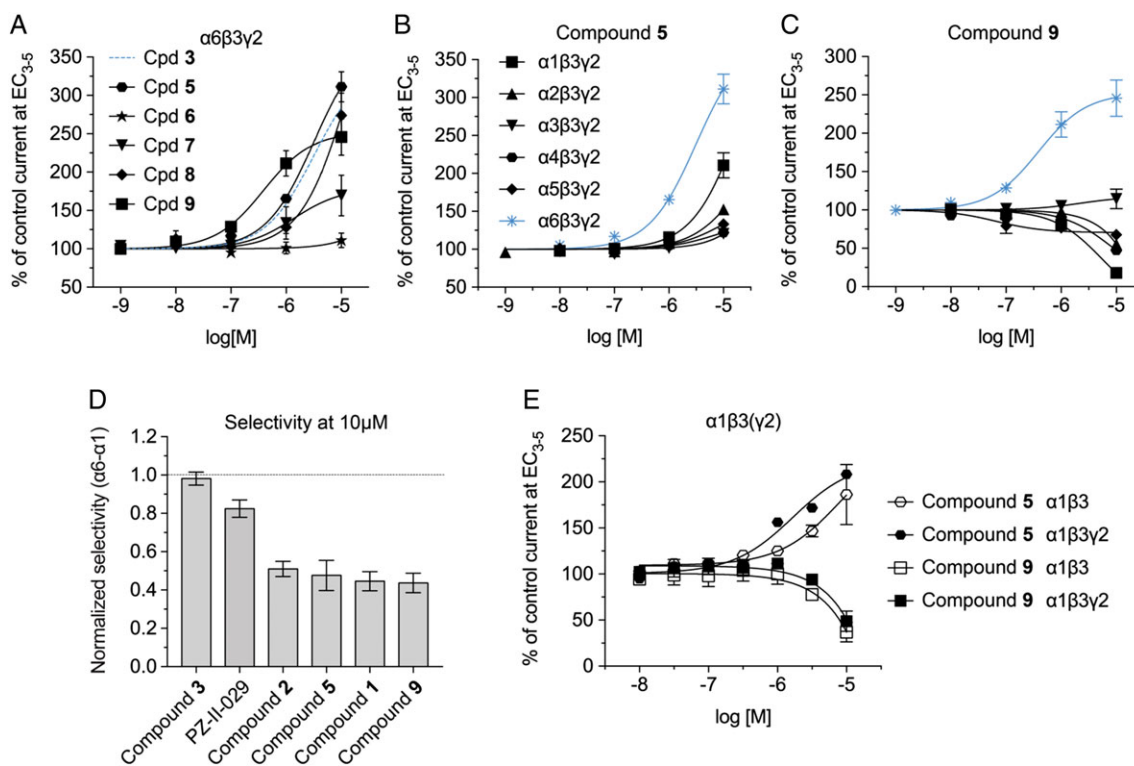
Figure 5

(A) Screening of a series of compounds **5–9** at α6β3γ2 GABAA receptors (see bottom row in Figure 1). At 1 μM compound concentration, compounds **3** (dashed blue line representing the fitted curve of Figure 2c), **5** and **9** show more than 150% modulation of GABA EC3–5 currents. At 10 μM compound concentrations, compounds **5**, **8** and **9** show strongest modulation of GABA EC3–5 currents, comparable to compound **3**. (B, C) Subunit profile of compounds **5** (B) and **9** (C) at αxβ3γ2 (x = 1–6) GABAA subunit combinations. Note that some receptors, particularly α1β3γ2, are positively modulated by compound **5** but negatively modulated by compound **9**. (D) Effective selectivity of 10 μM compound at α6β3γ2 over α1β3γ2. Modulation at α1β3γ2 was calculated as fraction of the modulation at α6β3γ2 [baseline (100%) = 0, efficacy at α6β3γ2 = 1; all signs positive] and subtracted from 1. (E) Separate experiment comparing effects of compound **5** and compound **9** at α1β3 versus α1β3γ2 receptors, demonstrating independence from the γ subunit.

Discussion

Previous work from our labs has identified several PQ compounds with strong preferential modulatory activity at α6β3γ2 over other αxβ3γ2 (x = 1–5) GABAA receptors, *via* the modulatory PQ binding site at the α+/β− interface (Varagic *et al.,* 2013a). However, the most α6-selective compound characterized in this earlier study, PZ-II-029 (R[7] = methoxy, *p*-methoxy), at 10 μM concentration still displays considerable residual modulatory activity of roughly 200% of control GABA currents in non-α6, αxβ3γ2 receptors (Varagic *et al.,* 2013a). We took the observation as a starting point for the present study that introducing a chloro substituent in position R[8] of the PQ compound **1** (resulting in compound **2**) greatly enhances efficacy while preserving relative modulatory activities at αxβ3γ2 (x = 1–5) receptors and preference for α6β3γ2. By systematically varying residues on ring D, we explored whether the subtype profile could be steered towards increased separation between α6− and other α-combinations. Indeed, we found that moving the methoxy residue from *p*- to *m*-position virtually abolished efficacy in all non-α6, αxβ3γ2 (x = 1–5) receptors. The resulting

compound **3**, at a concentration of 10 μM, retained around 300% modulation of control GABA currents at α6β3γ2 receptors and an estimated EC50 of 3.1 μM. Hence, compound **3**, to the best of our knowledge, displays the best α6/αx (x = 1–5) efficacy ratio in αxβ3γ2 (x = 1–6) GABAA receptors described to date.

Particular interest has recently developed for α6-containing GABAA receptors and their involvement in various diseases (Kramer and Bellinger, 2013; Liao *et al.,* 2016; Yang *et al.,* 2016). α6 subunits have a highly specific expression pattern in the central and peripheral nervous system. They are most abundantly found not only in CGCs but also in olfactory bulb, cochlear nucleus, hippocampus, trigeminal ganglion, sensory neurons and dorsal horn (Gutiérrez *et al.,* 1996; Puri *et al.,* 2012; Hörtnagl *et al.,* 2013; Yang *et al.,* 2016). Studies implicating α6-containing receptors in tic disorders (Liao *et al.,* 2016), depressive behaviours (Yang *et al.,* 2016) or inflammatory (Puri *et al.,* 2012) and myofascial pain of the trigeminal innervation area (Kramer and Bellinger, 2013) underscore the potential importance of selective compounds for α6-containing receptors, ideally exhibiting little to no residual effects *via* other GABAA receptor subtypes.

Selective positive modulators for α6-containing GABA$_A$ receptors might thus have future disease indications. The flavone hispidulin is a PAM at α6β2γ2S receptors, among other subtypes (Kavvadias *et al.*, 2004). It has been isolated from a plant extract and successfully used in a patient with intractable motor tic disorders (Huang *et al.*, 2015) and was found to specifically reduce metamphetamine-induced hyperlocomotion *via* cerebellar α6-GABA$_A$ receptors (Liao *et al.*, 2016). Interestingly, hispidulin did not interfere with spontaneous locomotor activity or motor coordination measured by rotarod performance. Looking beyond the cerebellum, considerable α6 subunit expression has also been found in trigeminal ganglion neurons and the brainstem trigeminal subnucleus caudalis of rats (Hayasaki *et al.*, 2006; Puri *et al.*, 2011, 2012; Kramer and Bellinger, 2013). Knockdown of α6 expression in the trigeminal ganglion using locally infused Gabrα6 siRNA aggravated the hypersensitivity associated with inflammatory temporomandibular joint arthritis (Puri *et al.*, 2012) and likewise increased myofascial nociception triggered by a ligature of the masseter muscle tendon (Kramer and Bellinger, 2013), supporting the notion that α6-containing GABA$_A$ receptors inhibit processing of nociceptive signals in the trigeminal pathway. These findings open up the possibility that positive modulators specific for α6-containing GABA$_A$ receptor might be suited to alleviate pain states of the trigeminal innervation area.

We found *o*-methoxy compound **4** to be devoid of positive modulatory activity at any receptor subunit combination tested. In fact, co-application with compound **3** suggests that compound **4** is a non-binder, rather than a silent binder, at α6β3γ2 receptors, rendering it a potentially useful negative control compound for future *in vivo* studies. Conformational analysis of compounds **2**, **3** and **4** revealed rotated dihedral angles between the plane surfaces of ring-system A–C and ring D in the case of compound **4**, suggesting that this difference in geometry might interfere with binding at the modulatory PQ binding site. In contrast, the binding affinity of compound **4** for the benzodiazepine binding site remained in the submicromolar range, suggesting that the dihedral angle of ring D might have a bigger impact on binding at the α+/β− site.

In a series of different *m*-substituents, we could not identify additional selective compounds with improved efficacy or potency in the α6β3γ2 receptor. However, two of those compounds, **5** and **9**, showed a curious pattern where *m*-methyl versus *m*-carboxy turns the former into a positive and the latter into a negative modulator of non-α6, αxβ3γ2 (*x* = 1–5) receptors, particularly at α1β3γ2. This finding is also the first demonstration of a negative modulatory effect mediated *via* the modulatory PQ site, as it is independent from the γ2 subunit and hence the BZD site. Additionally, we demonstrated that compound **3** does not require a γ2 subunit for current modulation, as it remains functionally α6-selective in αβδ receptor subtypes. Comparing compounds **5** and **9** with **3**, we observed three different modulatory effects at α1β3γ2 (**5** = PAM, **3** = null (silent) modulator or SAM and **9** = negative allosteric modulation), which seem to be induced by only the chemically different substituents in the *m*-position. Interestingly, positive allosteric modulation corresponds to an electron donating hydrophobic substituent (**5**, R$'^3$ = Me), whereas null modulation is observed for an electron

withdrawing hydrogen bond acceptor group (**3**, R$'^3$ = OMe) and negative modulation is induced by an electron withdrawing negatively ionizable group (**9**, R$'^3$ = COOH). These findings might prove useful for the design of new ligands and further structure–activity studies thereof. A systematic expansion along these lines may ultimately lead to structure–activity insights on efficacy selectivity and thus accelerate the targeted development of compounds with desired subtype profiles tremendously.

In summary, by systematically expanding on previously identified α6-preferring PQ compounds, we identified the highly α6β3γ2-selective compound **3**. This compound has a substitution pattern distinct from the so far best published α6β3γ2-selective PZ-II-029 [R^7-methoxy, *p*-methoxy; published as "compound 6" (Varagic *et al.*, 2013a)]. PZ-II-029 and compound **3** represent two separate prototypes for α6β3γ2-preferring PQs, differing in their ring A and D substitution patterns. Our present data are consistent with ring D substituents additionally determining efficacy selectivity for specific α-subunit-containing receptors. Future computational docking and functional studies are needed to determine the precise binding requirements for α-subunit specificity and efficacy determinants of this compound class. Furthermore, compound **3** could be used as tools to probe the functional role of α6β3γ2 GABA$_A$ receptors in cerebellar neuron cultures and brain slices, to complement existing heterologous data and future *in vivo* studies in disease models.

Acknowledgements

Author contributions

M.T. and D.C.B.S. contributed equally to this study. M.E., M.S. and M.D.M. participated in the design of the research. Experiments were conducted by M.T., D.C.B.S., K.B., R.H., L.W., Z.V., J.F., F.S. and P.S. Data analysis was performed by M.T., D.C.B.S., K.B., J.F., F.S. and P.S. All authors wrote or contributed to the writing of the manuscript.

Conflict of interest

The authors declare no conflicts of interest.

Declaration of transparency and scientific rigour

This Declaration acknowledges that this paper adheres to the principles for transparent reporting and scientific rigour of preclinical research recommended by funding agencies, publishers and other organisations engaged with supporting research.

References

Alexander SPH, Peters JA, Kelly E, Marrion NV, Faccenda E, Harding SD et al. (2017). The Concise Guide to PHARMACOLOGY 2017/18: Ligand-gated ion channels. Br J Pharmacol 174: S130–S159.

Bennett, D.A. (1987). Pharmacology of the pyrazolo-type compounds: agonist, antagonist and inverse agonist actions. Physiol Behav 41: 241–245.

Bennett DA, Amrick CL, Wilson DE, Bernard PS, Yokoyama N, Liebman JM (1985). Behavioral pharmacological profile of CGS 9895: a novel anxiomodulator with selective benzodiazepine agonist and antagonist properties. Drug Dev Res 6: 313–325.

Cooper SJ, Kirkham TC, Estall LB (1987). Pyrazolpquinolines: second generation benzodiazepine receptor ligands have heterogeneous effects. Trends Pharmacol Sci 8: 180–184.

Curtis MJ, Bond RA, Spina D, Ahluwalla A, Alexander SP, Giembycz MA et al. (2015). Experimental design and analysis and their reporting: new guidance for publication in BJP. Br J Pharmacol 172: 3461–3471.

Czernik AJ, Petrack B, Kalinsky HJ, Psychoyos S, Cash WD, Tsai C et al. (1982). CGS 8216: receptor binding characteristics of a potent benzodiazepine antagonist. Life Sci 30: 363–372.

Ernst M, Brauchart D, Boresch S, Sieghart W (2003). Comparative modeling of GABA$_A$ receptors: limits, insights, future developments. Neuroscience 119: 933–943.

File SE (1983). Proconvulsant action of CGS 8216. Neurosci Lett 35: 317–320.

Forkuo GS, Guthrie ML, Yuan NY, Nieman AN, Kodali R, Jahan R et al. (2016). Development of GABA$_A$ receptor subtype-selective imidazobenzodiazepines as novel asthma treatments. Mol Pharm 13: 2026–2038.

Fryer RI, Zhang P, Rios R, Gu ZQ, Basile AS, Skolnick P (1993). Structure-activity relationship studies at the benzodiazepine receptor (BZR): a comparison of the substitutent effects of pyrazoloquinolinone analogs. J Med Chem 36: 1669–1673.

Gee KW, Yamamura HI (1982). A novel pyrazoloquinoline that interacts with brain benzodiazepine receptors: characterization of some in vitro and in vivo properties of CGS 9896. Life Sci 30: 2245–2252.

Gutiérrez A, Khan ZU, De Blas AL (1996). Immunocytochemical localization of the alpha 6 subunit of the gamma-aminobutyric acidA receptor in the rat nervous system. J Comp Neurol 365: 504–510.

Hayasaki H, Sohma Y, Kanbara K, Maemura K, Kubota T, Watanabe M (2006). A local GABAergic system within rat trigeminal ganglion cells. Eur J Neurosci 23: 745–757.

Hörtnagl H, Tasan RO, Wieselthaler A, Kirchmair E, Sieghart W, Sperk G (2013). Patterns of mRNA and protein expression for 12 GABA$_A$ receptor subunits in the mouse brain. Neuroscience 236: 345–372.

Huang WJ, Lee HJ, Chen HL, Fan PC, Ku YL, Chiou LC (2015). Hispidulin, a constituent of Clerodendrum inerme that remitted motor tics, alleviated methamphetamine-induced hyperlocomotion without motor impairment in mice. J Ethnopharmacol 166: 18–22.

Jechlinger M, Pelz R, Tretter V, Klausberger T, Sieghart W (1998). Subunit composition and quantitative importance of hetero-oligomeric receptors: GABA$_A$ receptors containing alpha6 subunits. J Neurosci 18: 2449–2457.

Kavvadias D, Sand P, Youdim KA, Qaiser MZ, Rice-Evans C, Baur R et al. (2004). The flavone hispidulin, a benzodiazepine receptor ligand with positive allosteric properties, traverses the blood-brain barrier and exhibits anticonvulsive effects. Br J Pharmacol 142: 811–820.

Kilkenny C, Browne W, Cuthill IC, Emerson M, Altman DG (2010). Animal research: reporting in vivo experiments: the ARRIVE guidelines. Br J Pharmacol 160: 1577–1579.

Kolata G (1982). New valiums and anti-valiums on the horizon. Science 216: 604–605.

Kramer PRR, Bellinger LLL (2013). Reduced GABA$_A$ receptor α6 expression in the trigeminal ganglion enhanced myofascial nociceptive response. Neuroscience 245: 1–11.

Liao Y-H, Lee H-J, Huang W-J, Fan P-C, Chiou L-C (2016). Hispidulin alleviated methamphetamine-induced hyperlocomotion by acting at α6 subunit-containing GABA$_A$ receptors in the cerebellum. Psychopharmacology (Berl) 233: 3187–3199.

Maldifassi MC, Baur R, Sigel E (2016). Molecular mode of action of CGS 9895 at α1 β2 γ2 GABA$_A$ receptors. J Neurochem 138: 722–730.

McGrath JC, Lilley E (2015). Implementing guidelines on reporting research using animals (ARRIVE etc.): new requirements for publication in BJP. Br J Pharmacol 172: 3189–3193.

Minier F, Sigel E (2004). Positioning of the alpha-subunit isoforms confers a functional signature to gamma-aminobutyric acid type A receptors. Proc Natl Acad Sci U S A 101: 7769–7774.

Olsen RW, Sieghart W (2008). International Union of Pharmacology. LXX. Subtypes of gamma-aminobutyric acid(A) receptors: classification on the basis of subunit composition, pharmacology, and function. Update. Pharmacol Rev 60: 243–260.

Puri J, Bellinger LL, Kramer PR (2011). Estrogen in cycling rats alters gene expression in the temporomandibular joint, trigeminal ganglia and trigeminal subnucleus caudalis/upper cervical cord junction. J Cell Physiol 226: 3169–3180.

Puri J, Vinothini P, Reuben J, Bellinger LL, Ailing L, Peng YB et al. (2012). Reduced GABA(A) receptor α6 expression in the trigeminal ganglion alters inflammatory TMJ hypersensitivity. Neuroscience 213: 179–190.

Puthenkalam R, Hieckel M, Simeone X, Suwattanasophon C, Feldbauer RV, Ecker GF et al. (2016). Structural studies of GABA$_A$ receptor binding sites: which experimental structure tells us what? Front Mol Neurosci 9: 1–20.

Ramerstorfer J, Furtmüller R, Sarto-Jackson I, Varagic Z, Sieghart W, Ernst M et al. (2011). The GABA$_A$ receptor alpha+beta− interface: a novel target for subtype selective drugs. J Neurosci 31: 870–877.

Savini L, Chiasserini L, Pellerano C, Biggio G, Maciocco E, Serra M et al. (2001). High affinity central benzodiazepine receptor ligands. Part 2: quantitative structure-activity relationships and comparative molecular field analysis of pyrazolo[4,3-c]quinolin-3-ones. Bioorg Med Chem 9: 431–444.

Sieghart W, Schuster A (1984). Affinity of various ligands for benzodiazepine receptors in rat cerebellum and hippocampus. Biochem Pharmacol 33: 4033–4038.

Sieghart W, Ramerstorfer J, Sarto-Jackson I, Varagic Z, Ernst M (2012). A novel GABA(A) receptor pharmacology: drugs interacting with the α(+) β(−) interface. Br J Pharmacol 166: 476–485.

Sigel E (2002). Mapping of the benzodiazepine recognition site on GABA(A) receptors. Curr Top Med Chem 2: 833–839.

Simeone X, Siebert DCB, Bampali K, Varagic Z, Treven M, Rehman S et al. (2017). Molecular tools for GABA$_A$ receptors: High affinity ligands for β1-containing subtypes. Sci Rep 7: 5674.

Southan C, Sharman JL, Benson HE, Faccenda E, Pawson AJ, Alexander SPH et al. (2016). The IUPHAR/BPS guide to PHARMACOLOGY in 2016: towards curated quantitative interactions between 1300 protein targets and 6000 ligands. Nucl Acids Res 44: D1054–D1068.

Valenzuela CF, Jotty K (2015). Mini-review: effects of ethanol on GABA$_A$ receptor-mediated neurotransmission in the cerebellar cortex – recent advances. Cerebellum 14: 438–446.

Varagic Z, Ramerstorfer J, Huang S, Rallapalli S, Sarto-Jackson I, Cook J et al. (2013a). Subtype selectivity of α+β− site ligands of GABA$_A$ receptors: identification of the first highly specific positive modulators at α6β2/3γ2 receptors. Br J Pharmacol 169: 384–399.

Varagic Z, Wimmer L, Schnürch M, Mihovilovic MD, Huang S, Rallapalli S et al. (2013b). Identification of novel positive allosteric modulators and null modulators at the GABA$_A$ receptor α+β− interface. Br J Pharmacol 169: 371–383.

Yang L, Xu T, Zhang K, Wei Z, Li X, Huang M et al. (2016). The essential role of hippocampal alpha6 subunit-containing GABA$_A$ receptors in maternal separation stress-induced adolescent depressive behaviors. Behav Brain Res 313: 135–143.

Yokoyama N, Ritter B, Neubert AD (1982). 2-Arylpyrazolo[4,3-c] quinolin-3-ones: novel agonist, partial agonist, and antagonist of benzodiazepines. J Med Chem 25: 337–339.

Supporting Information

Additional Supporting Information may be found online in the supporting information tab for this article.

https://doi.org/10.1111/bph.14087